



OPEN The copper chelator ammonium tetrathiomolybdate inhibits the progression of experimental endometriosis in TNFR1-deficient mice

Rocío Ayelem Conforti, María Belén Delsouc✉, Ana Sofia Zabala, Sandra Silvina Vallcaneras & Marilina Casais✉

The TNF- α /TNFR system is involved in endometriosis (EDT), a gynecologic estrogen-dependent disease. Elevated copper concentrations have also been associated with EDT, even in TNFR1-deficient mice where disease worsening occurs. We aimed to evaluate whether treatment with ammonium tetrathiomolybdate (TM, copper chelator) is beneficial in TNFR1-deficient mice presenting with worsened EDT status. Female C57BL/6 mice were divided into three groups: KO Sham, KO EDT, and KO EDT+TM. TM was administered from the 15th postoperative day, and samples were collected one month after inducing pathology. In peritoneal fluid, copper and estradiol levels were determined by electrothermal atomic absorption spectrometry and electrochemiluminescence, respectively. Lesions were processed for the analysis of cell proliferation (PCNA immunohistochemistry), expression of angiogenic markers (RT-qPCR), and oxidative stress (spectrophotometric methods). We found that EDT increased copper and estradiol levels compared to the KO Sham group, while the TM administration restored the levels of both factors. TM also reduced the volume and weight of the lesions and cell proliferation rate. Besides, TM treatment decreased the number of blood vessels and the *Vegfa*, *Fgf2*, and *Pdgfb* expression. Furthermore, superoxide dismutase and catalase activity decreased, and lipid peroxidation increased. TM administration inhibits EDT progression in TNFR1-deficient mice where the pathology is exacerbated.

Endometriosis (EDT) is a chronic estrogen-dependent disease characterized by the growth of endometrial-like tissue outside the uterus. EDT is currently considered a systemic disease and affects 5–10% of reproductive-age patients in the world¹. It usually causes severe pelvic pain, heavy bleeding, dysmenorrhea, and subfertility, which can compromise the life quality of patients².

Several studies on EDT have reported the crucial role played by the tumor necrosis factor- α (TNF- α) and its receptors (TNFR1 and TNFR2)^{3–6}. TNFR1 (TNFRp55) is constitutively expressed in almost all cell types. Its activation leads to pro-inflammatory pathways and programmed cell death. In contrast, TNFR2 (TNFRp75) is expressed on limited cells, such as immune cells, endothelial cells, neural cells, and even some tumor cells^{7–9}. This receptor has been shown to mediate signals that promote tissue repair, proliferation, and angiogenesis^{9,10}. Cell survival, cell proliferation, and death occur as a balance between the TNFR1 and TNFR2 signaling pathways, demonstrating the significant crosstalk between them^{8,10}. In this regard, it has been postulated that in healthy women, endometrial cells do not implant in ectopic sites because TNF- α activates cell death through TNFR1 and inhibits cell proliferation by down-regulating TNFR2⁴. Interestingly, low TNFR1 expression was reported in women with EDT during the late secretory phase, which could favor the survival and growth of menstrual debris outside the uterus^{11,12}. In another study in patients, TNFR1 levels were shown to increase and then decrease from minimal to severe stages of the disease. In contrast, the TNFR2 levels and TNF- α increased as EDT worsened¹³.

Facultad de Química, Bioquímica y Farmacia, Universidad Nacional de San Luis (UNSL). Instituto Multidisciplinario de Investigaciones Biológicas de San Luis (IMIBIO-SL-CONICET), D5700HHW San Luis, Argentina. ✉email: mbdelsouc@unsl.edu.ar; mcasais@unsl.edu.ar

We previously showed that, in TNFR1-deficient mice, a worsening of pathology is observed compared to the EDT progression in wild-type mice^{5,6,14}.

Elevated Cu levels have been reported in serum and urine samples from women with EDT^{15,16}. This metal has been associated with oxidative stress in this pathology¹⁵, a process that possibly contributes to the malignant transformation of EDT¹⁷. Cu homeostasis has also been shown to be dysregulated in many cancers¹⁸. Cu can act as a pro-angiogenic metal by modulating the expression of vascular endothelial growth factor (VEGF), fibroblast growth factor 2 (FGF-2), and cytokines¹⁹. In addition, TNF- α secretion can also be regulated by Cu in cancer cells¹⁹, and it has been reported that TNFR1 activation can mediate the cytotoxic effects of the metal^{20,21}. Being a metalloestrogen, Cu can also potentiate the estrogenic action, estradiol-induced tumor cell proliferation²² and, at high levels, stimulate the expression of enzymes involved in estradiol synthesis²³.

There is no cure for EDT; especially, hormone therapy is only partially effective and often has significant side effects, limiting its long-term use²⁴. Since none of the current treatments are guaranteed to work in EDT, the pathophysiological implication of the TNF- α /TNFR system highlights the need to study potential new therapies that may be useful for patients with this unbalanced situation²⁵. Recently, we demonstrated that the ammonium tetrathiomolybdate (TM) administration to EDT-induced wild-type mice affects the progression of pathology²⁶. TM is a fast-absorbing, low-toxicity Cu chelator that was initially developed as a treatment for Wilson's disease²⁷ but has also shown anti-proliferative and anti-angiogenic effects in several cancers^{28,29}. TM interferes with the activity of numerous cuproenzymes and nuclear factor κ B (NF- κ B), leading to lower VEGF, FGF-2, and cytokines²⁸. Therefore, considering the involvement of the TNF- α /TNFR system and Cu in the EDT, in the present work, we administered TM in mice to evaluate whether copper chelation is beneficial in a TNFR1^{-/-} worsened EDT status.

Results

Experimental EDT increased Cu levels in the peritoneal fluid of TNFR1^{-/-} mice, while the administration of TM restored the concentration of this metal. Due to the implication of Cu in the EDT progression, we used a chelator and, therefore, we analyzed the levels of the metal in the peritoneal fluid of all experimental animals. On the one hand, the establishment of the pathology (KO EDT group) produced an increase in Cu concentration compared to the KO Sham group ($P < 0.001$; Fig. 1). On the other hand, the administration of TM significantly decreased the concentration of this metal ($P < 0.001$; Fig. 1), reaching values similar to those of the KO Sham group.

TM affected the development of endometriotic-like lesions in TNFR1-deficient mice. We found that there were no statistically significant differences in the number of lesions established per mouse between experimental groups (Fig. 2a). However, TM administration caused a decrease in both lesion volume ($P < 0.01$, Fig. 2b) and lesion weight ($P < 0.001$, Fig. 2c) compared to the KO EDT group.

TM modulated estradiol levels in TNFR1-deficient mice. Since EDT is an estrogen-dependent disease, estradiol levels in the peritoneal fluid were analyzed. On the one hand, the induction of the pathology produced a significant increase in the levels of this hormone compared to the Sham group ($P < 0.001$; Fig. 3a). On the other hand, TM administration significantly decreased estradiol concentration ($P < 0.001$; Fig. 3a), reaching values similar to those of the KO Sham group. It should be noted that a correlation study demonstrated a moderate positive correlation between the volume of the lesion and estradiol levels ($P < 0.05$; Fig. 3b).

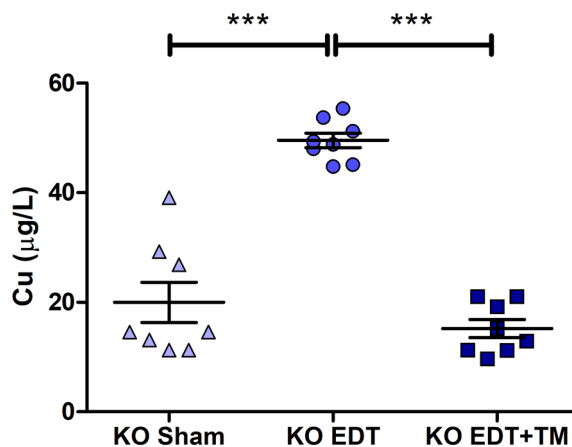


Figure 1. Effect of TM on the Cu concentration in the peritoneal fluid of TNFR1^{-/-} mice. Cu was determined by ETAAS in sham-operated mice (KO Sham; triangles), EDT-induced mice (KO EDT; circles), and TM-treated EDT-induced mice (KO EDT+TM; squares). Results are expressed as mean \pm SEM ($n = 8$ animals/group). One-way ANOVA followed by Tukey's test was used. *** $P < 0.001$.

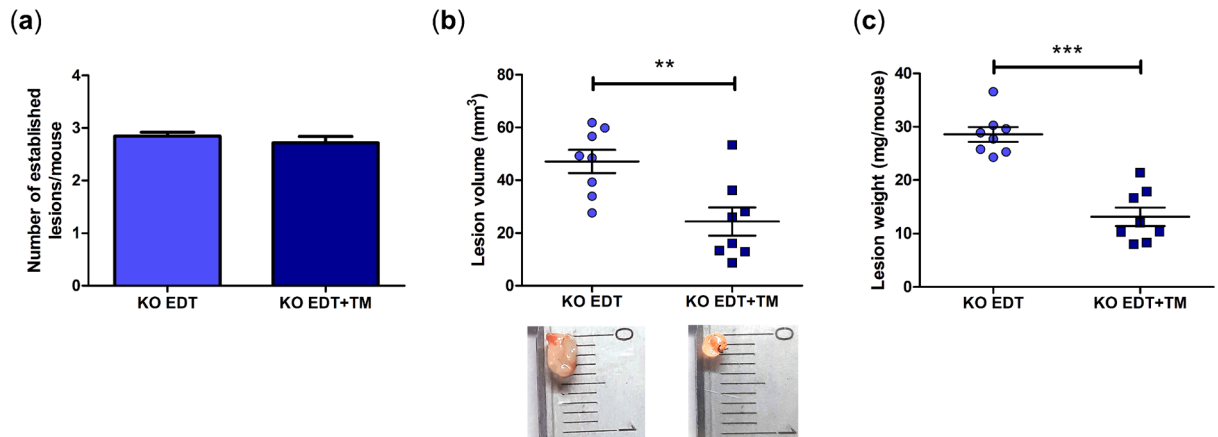


Figure 2. Effect of TM on the development of endometriotic-like lesions in $TNFR1^{-/-}$ mice. The number of established lesions (a), their volume (b), and their weight (c) were evaluated in EDT-induced mice (KO EDT) and TM-treated EDT-induced mice (KO EDT+TM) after one month of inducing the pathology. Representative images of the morphology of endometriotic-like lesions are provided. Results are expressed as mean \pm SEM ($n=8$ animals/group). KO EDT: circles; KO EDT+TM: squares. Statistical comparisons were made using Student's t test. ** $P<0.01$; *** $P<0.001$.

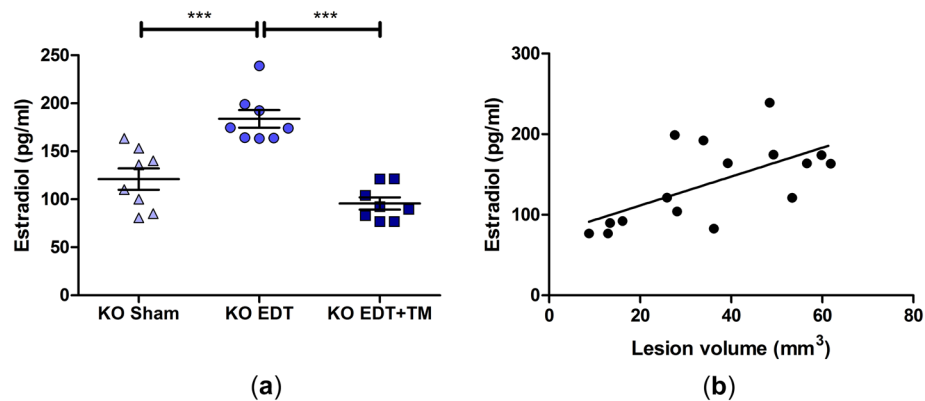


Figure 3. Effect of TM on the estradiol levels in the peritoneal fluid of $TNFR1^{-/-}$ mice. Estradiol was analyzed by ECLIA in sham-operated mice (KO Sham; triangles), EDT-induced mice (KO EDT; circles), and TM-treated EDT-induced mice (KO EDT+TM; squares) (a). Results are expressed as mean \pm SEM ($n=8$ animals/group). One-way ANOVA followed by Tukey's test was used. *** $P<0.001$. In addition, a correlation study between the lesion volume and estradiol was performed for the entire group of mice with EDT ($n=16$) (b). The normality of data was assessed with the Shapiro–Wilk test, and Spearman's correlation method was applied. * $P<0.05$, Spearman $r=0.5548$.

Treatment with TM decreased the cell proliferation in $TNFR1$ -deficient endometriotic-like lesions. Based on the anti-proliferative capacity of TM, we analyzed the PCNA labeling index in lesions sections by immunohistochemistry. Histologically, endometriotic-like lesions from untreated mice showed endometrial glands and abundant stroma, a typical structure consistent with their endometrial origin (Fig. 4a). TM administration notably reduced these EDT histopathological marks (Fig. 4b). This Cu chelator reduced the percentage of PCNA-positive cells ($P<0.001$; Fig. 4c) compared to the lesions from untreated $TNFR1$ -deficient animals (KO EDT group), in correspondence with the lower weight and volume of the lesions found in the KO EDT+TM group.

Cu chelation decreased the number of blood vessels and the mRNA expression of *Vegfa*, *Fgf2*, and *Pdgfb* in endometriotic-like lesions. The importance of angiogenesis for the sustained development of endometriotic lesions is well known. Different studies suggest that TM can interfere with this process. Therefore, we evaluated its effect in our experimental EDT $TNFR1$ -deficient model. On the one hand, we were able to observe in sections of endometriotic-like lesions stained with hematoxylin–eosin (Fig. 5a) that TM significantly decreased the number of blood vessels ($P<0.01$; Fig. 5b). On the other hand, this Cu chelator also reduced the mRNA expression of *Vegfa* ($P<0.05$; Fig. 5c), *Fgf2* ($P<0.05$; Fig. 5d), and *Pdgfb* ($P<0.05$; Fig. 5e) compared to the KO EDT group.

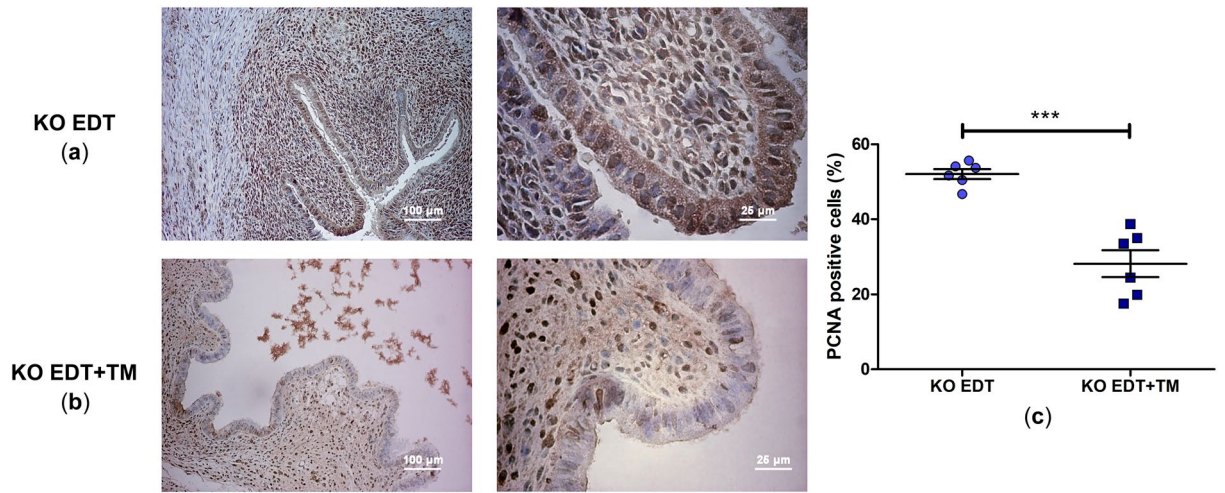


Figure 4. Effect of TM on cell proliferation of endometriotic-like lesions in $TNFR1^{-/-}$ mice. The micrographs show representative histological sections of induced endometriotic-like lesions (magnification: $100\times$ and $400\times$) in untreated mice (KO EDT) (a) and TM-treated mice (KO EDT+TM) (b). Scale bar, $100\ \mu\text{m}$ and $25\ \mu\text{m}$, respectively. The percentage of proliferating cells in endometriotic-like lesions was evaluated by immunohistochemistry for PCNA in both experimental groups (c). PCNA-positive cells were identified by the presence of brown nuclear reactivity. Results are expressed as mean \pm SEM ($n=6$ animals/group). KO EDT: circles; KO EDT+TM: squares. Statistical comparisons were made using Student's t test. *** $P < 0.001$.

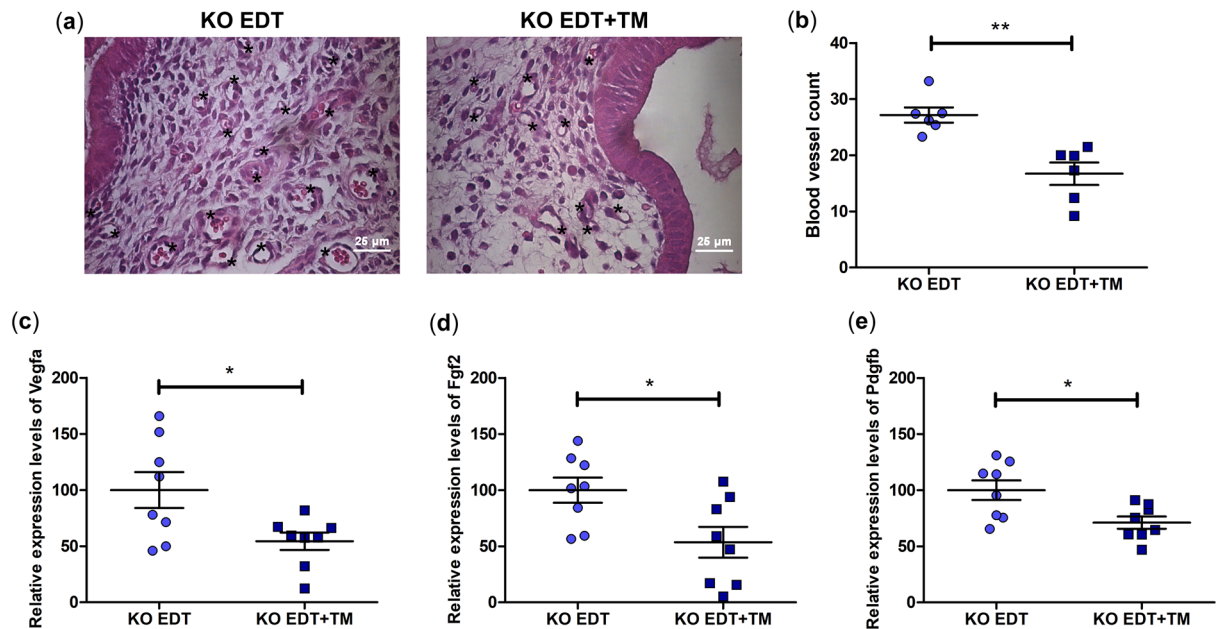


Figure 5. Effect of TM on the angiogenic process in endometriotic-like lesions in $TNFR1^{-/-}$ mice. The micrographs show representative histological sections of endometriotic-like lesions induced in untreated (KO EDT) and TM-treated (KO EDT+TM) mice (a). Blood vessels of different calibers are marked with an asterisk. Magnification: $400\times$. Scale bar, $25\ \mu\text{m}$. The counting of blood vessels was performed on sections stained with hematoxylin–eosin using an optical light microscope for both experimental groups (b). Results are expressed as mean \pm SEM ($n=6$ animals/group). The mRNA expression of *Vegfa* (c), *Fgf2* (d), and *Pdgfb* (e) in endometriotic-like lesions was evaluated for both experimental groups. The relative quantification of each mRNA was calculated from the C_q values obtained for the genes of interest and the reference gene (*Rn18s*) using the $2^{-\Delta\Delta C_t}$ method. Results are expressed as mean \pm SEM ($n=8$ animals/group). KO EDT: circles; KO EDT+TM: squares. Statistical comparisons were made using Student's t test. * $P < 0.05$; ** $P < 0.01$.

TM decreased the SOD and CAT activity and increased the lipid peroxidation in endometriotic-like lesions of TNFR1-deficient mice. Cu is an integral part of many important enzymes and is a redox-active metal. Therefore, we evaluate the effect of TM on antioxidant enzymatic defenses. We observed that this Cu chelator decreased the SOD activity ($P < 0.05$; Fig. 6a) and CAT activity ($P < 0.05$; Fig. 6b) but did not change GPX activity (Fig. 6c) in endometriotic-like lesions compared to the KO EDT group. In addition, we analyzed TBARS-MDA, a biomarker of lipid oxidation. TM significantly increased the MDA concentration in endometriotic-like lesions concerning the KO EDT group ($P < 0.001$; Fig. 6d), showing that this drug modifies the oxidative status.

Discussion

In different studies, it has been observed that the TNF- α /TNFR system and Cu are involved in the EDT progression^{3-6,15,16}. Therefore, in this work, we evaluated the therapeutic potential of Cu chelation by TM in a TNFR1^{-/-} worsened EDT status in mice. Under these experimental conditions, we found increased levels of Cu in the peritoneal fluid. TM reduced the levels of this metal to physiological concentrations without compromising animal welfare. This ‘old drug’ has been repositioned for cancer some years ago due to its anti-proliferative and anti-angiogenic effects in animal models and clinical studies^{28,29}. Although EDT is not cancer in itself, it exhibits similar characteristics: progressive and invasive growth, recurrence, and a tendency to metastasize and develop its blood supply³⁰, which prevail in animal models of the pathology and in conditions of imbalance of the TNF- α /TNFR system⁵. Based on this, we analyzed the effect of the administration of this drug in the experimental EDT induced in TNFR1^{-/-} mice.

Regarding the volume of the lesions, in TNFR1-deficient animals, the values obtained are higher than those previously reported in wild-type animals²⁶, showing similarity with that reported by Vallcaneras et al.⁵. Therefore, our results continue to support that TNFR1 deficiency exacerbates EDT. According to Vallcaneras et al., this worsening of the pathology is due, among other factors, to a decrease in cell death and an increase in proliferation⁵. The observed increase in the size of the lesions is probably due to the activation of TNFR2-dependent pathways. The involvement of TNFR2 in various tumor cell types has been demonstrated³¹, promoting tumor growth through signal transduction cascades such as the Akt signaling pathway and the NF- κ B induction through p42/p44 mitogen-activated protein kinase (MAPK)/ERK pathway⁸. In addition, blockade of TNFR2 has been shown to decrease tumor growth³² and EDT development³³, which would indicate that this receptor is more necessary for the progression of proliferative diseases than the activation of p42/p44 MAPK/ERK and Akt through TNFR1. Therefore, we evaluated whether TM treatment affected *Tnfr2* mRNA expression. We observed this Cu chelator significantly reduced *Tnfr2* expression in endometriotic-like lesions (Supplementary Fig. S1). Importantly, TM treatment affected the volume and weight of lesions induced in TNFR1^{-/-} mice. This fact could be associated with the Cu levels decrease since this metal can stimulate the aforementioned signaling pathways^{34,35}, among other effects, which define it as a factor that promotes tumor progression. Supporting all of the above, we found that this Cu chelator reduced cell proliferation rate compared to lesions in the KO EDT group.

Furthermore, we showed that in EDT-induced KO animals, the development of this disease increased estradiol levels in peritoneal fluid. It is known that Cu can modulate steroidogenesis: at low levels, it can decrease serum dehydroepiandrosterone (DHEA)³⁶, a precursor of estradiol along with cholesterol, while at high levels, it can stimulate the expression of enzymes involved in estradiol synthesis²³. Indeed, we determined that the Cu chelation with TM restored estradiol levels in the peritoneal fluid. We also demonstrated a positive correlation between estradiol levels and the volume of endometriotic-like lesions. This fact supports once again that EDT is an estrogen-dependent disease¹. Interestingly, like TNFR2 and Cu, estradiol promotes tumor growth and cell proliferation^{8,34,35,37}. In this sense, the TM action on Cu and estradiol levels in our experimental model, as well as its recognized ability to prevent the activation of signaling pathways that drive cell proliferation^{38,39}, could justify its efficacy in reducing lesion development even in the absence of TNFR1.

Along with cell proliferation, the establishment of new blood vessels is essential for endometriotic lesions to develop⁴⁰. We have previously observed anti-angiogenic effects of TM in EDT-induced wild-type mice, which hampered the progression of the pathology²⁶. In the present study with TNFR1^{-/-} mice, we observed that treatment with TM reduced the number of blood vessels and the mRNA expression of the three pro-angiogenic factors analyzed (*Vegf*, *Fgf2*, and *Pdgfb*). It is argued that the combined inhibition of VEGF, FGF-2, and PDGF-B would be very effective in suppressing the vascularization of endometriotic lesions⁴¹; in fact, our results support

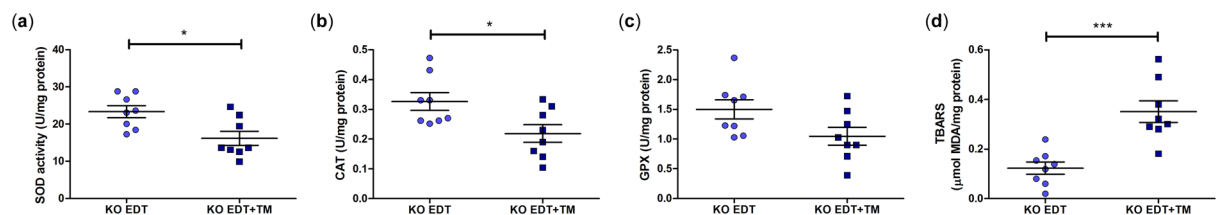


Figure 6. Effect of TM on oxidative stress in endometriotic-like lesions of TNFR1^{-/-} mice. The activity of the antioxidant enzymes SOD (a), CAT (b), and GPX (c) and the levels of MDA (d) were analyzed in lesions of untreated mice (KO EDT; circles) and TM-treated mice (KO EDT+TM; squares). Results are expressed as mean \pm SEM (n = 8 animals/group). Statistical comparisons were made using Student's *t* test. * $P < 0.05$; *** $P < 0.001$.

the above. The decrease in the expression of the pro-angiogenic factors analyzed may be because TM inhibits the activation of NF- κ B^{28,42}. On the one hand, TM affects the phosphorylation and consequent degradation of I κ B α , the major inhibitory protein of NF- κ B⁴³. On the other hand, TM decreases the expression of inhibitors of apoptosis proteins (IAP family)^{44,45}, which are increased in EDT⁴⁶ and are required for NF- κ B activation through TNFR1 and TNFR2⁴⁷. In our experimental TNFR1^{-/-} research design, we have shown that TM decreases the expression of *Tnfr2* mRNA. Taking all of the above into account, it is likely that TM has a strong inhibitory action on NF- κ B in these deficient animals, compromising key downstream pathways for EDT progression. It is supported by the fact that, unlike what was observed in wild-type animals²⁶, the Cu chelator administration, besides reducing the expression of *Fgf2* and *Pdgfb*, significantly reduced the *Vegfa* expression, being effective in this worsened state of the pathology. It is important to mention that, in the absence of TNFR1, all TNFR2-dependent pathways become relevant, particularly those related to cell proliferation, survival, and angiogenesis⁸. In fact, in a previous study carried out in TNFR1^{-/-} animals, it was found that there was greater activation of NF- κ B than in wild-type animals¹⁴. Therefore, we postulate that, in the absence of TNFR1, there is not only an interruption of the recognized crosstalk between both TNFRs¹⁰ but also an alteration of TNFR2 signaling by TM. In addition to the above, TM has been shown to inhibit SOD1 enzyme activity, thereby affecting angiogenesis and inducing vessel abnormalities⁴⁸, possibly by downregulating PDGFR⁴⁹.

Deregulation of antioxidant defenses leads to the establishment of a pro-oxidant environment in proliferative diseases. In this regard, an increase in SOD activity and a decrease in CAT activity have been described in EDT, associated with an increase in the production of reactive oxygen species (ROS)⁵⁰. Among the ROS is hydrogen peroxide, which acts as a second messenger in cell signaling to maintain an EDT-associated proliferative phenotype⁵¹. However, the overproduction of ROS can also promote cell damage. Delsouc et al. reported that in TNFR1^{-/-} mice with induced EDT, antioxidant protection increases in the peritoneal cavity with respect to the wild-type group, supporting the exacerbation of the disease⁶. Here we observe that TM administration decreases SOD and CAT activity, possibly tipping the balance towards ROS-induced apoptotic signaling. Our assumption is supported by the reduced volume of lesions and increased MDA concentration in these tissues, suggesting oxidative damage. While the increase in SOD activity has been postulated as a compensatory mechanism to control the increase in oxidative stress in EDT, its inhibition has been shown to induce an oxidative burst that produces cell and tissue damage⁵⁰. The decrease in SOD activity could be due to the ability of TM to remove Cu ions from the active site of SOD1⁵². Moreover, TM could be indirectly responsible for the reduction of CAT activity by affecting the dismutation of the superoxide radicals to molecular oxygen and hydrogen peroxide; the latter is converted by CAT in molecular oxygen and water. This fact would reinforce the induction of the oxidative burst. SOD1 is more than an antioxidant enzyme; its inhibition by TM contributes to attenuating angiogenesis and tumor cell proliferation⁴⁸. In fact, all of these processes were compromised in our TNFR1-deficient experimental model after the drug administration period, preventing EDT progression.

In summary, TM administration inhibits EDT progression in TNFR1^{-/-} mice, in which the pathology is aggravated. Given the loss of Cu homeostasis in this complex pathology, our preclinical evidence in a situation of imbalance in the TNF- α /TNFR system suggests that TM has therapeutic potential. This drug needs to continue to be evaluated in different EDT experimental research designs for possible repositioning.

Methods

Two-month-old female TNFR1^{-/-} C57BL/6 mice, weighing 19–21 g, were used. Animals were housed in the Universidad Nacional de San Luis Animal Facility (San Luis, Argentina) under strict light conditions (12 h light, 12 h darkness), controlled temperature (22 \pm 2 °C), sterile water, and ad libitum feeding. All experimental procedures were performed following the Guide for the Care and Use of Laboratory Animals of the National Research Council (8th ed., 2011, Washington, DC) and complied with the ARRIVE guidelines 2.0. This study was reviewed and approved by the Comité Institucional de Cuidado y Uso de Animales (CICUA) of the Universidad Nacional de San Luis (Protocols No. B-304/20 and B-304/21).

Experimental design. Twenty-four TNFR1^{-/-} mice (KO) were randomly divided into three groups: (1) sham-operated mice (KO Sham), (2) EDT-induced mice (KO EDT), and (3) TM-treated EDT-induced mice (KO EDT+TM). The EDT induction consisted of autologous uterine tissue transplantation to the intestinal mesentery^{5,26}. For this, animals were anesthetized with an intraperitoneal injection of ketamine-xylazine: 100 mg/kg of ketamine and 10 mg/kg of xylazine (Holliday Scott, Buenos Aires, Argentina, and Richmond, Buenos Aires, Argentina, respectively). After a mid-ventral incision, the right uterine horn was removed from the animal, divided longitudinally, and then cut into four mm² pieces. The fragments were sutured in the intestinal mesentery with a 6-0 nylon suture to simulate endometriotic lesions. In Sham mice, three sutures were made without implanting uterine tissue. The mice's body weight, food consumption, and grooming behavior were monitored daily. One month after inducing EDT, animals were euthanized by cervical dislocation. Immediately, a small mid-ventral orifice was opened, through which 1.5 mL of pH 7.4 phosphate-buffered saline (PBS) was injected into the peritoneal cavity of each animal. Peritoneal lavage fluid was collected and centrifuged at 250 g for 10 min at 4 °C. Supernatants (*peritoneal fluid*) were collected and stored at -80 °C for Cu and estradiol determination. Finally, the abdomen of the EDT-induced animals was fully opened to access the endometriotic-like lesions.

Administration of TM. Starting on postoperative day 15 (period required for lesion establishment), each animal in the KO EDT+TM group received 0.3 mg of TM (cat# 323446, Sigma-Aldrich, St Louis, MO, USA) orally, as previously described²⁶. Weekly controls of body weight and hematocrit were performed to ensure that

severe Cu deficiency did not occur^{42,53}. Furthermore, no toxicity evidence was observed for the administered dose based on food consumption or grooming behavior compared to the KO Sham and KO EDT groups.

Cu determination. Cu concentration in the peritoneal fluid was determined by electrothermal atomic absorption spectrometry (ETAAS) with a graphite furnace. Peritoneal fluid samples (500 μ L) were mineralized with 500 μ L concentrated nitric acid and 500 μ L hydrogen peroxide. After adding the solutions, transparent samples were obtained by heating at 60 °C for 1 h in a thermostated water bath. All samples and reagents were prepared in 15 mL metal-free polypropylene tubes (Sarstedt, Germany). The reagents used were of trace analysis grade. They included: Ultrapure water with a resistivity of 18.2 M Ω cm produced by an Easy pure RF system from Barnstead (Dubuque, IA, USA), Double distilled acids obtained with a PTFE sub-boiling acid distiller (Distillacid, Berghof Products+Instruments GmbH, Germany) and 30% hydrogen peroxide (Merck, Germany). A Shimadzu Model AA-7000 atomic absorption spectrometer (Tokyo, Japan) was used to perform the measurements, equipped with a GFA-EX7 atomizer and an ASC-6100 autosampler. Integrated platform graphite tubes (Lvov), Shimadzu (Tokyo, Japan), were used in all experiments. A Cu hollow cathode lamp (Hamamatsu, Photonics, K.K., Japan) was employed as a radiation source at 324.8 nm with a 0.5 nm slit. All measurements were performed in duplicate. The results were expressed in μ g/L.

Macroscopic analysis of the endometriotic-like lesions. Lesions were identified, counted, and measured with a caliper at two different perpendicular diameters. For the volume calculation, the following equation was used: $V = (4/3) \pi r_1^2 r_2$ (r_1 and r_2 are the radiuses and $r_1 < r_2$). Subsequently, the lesions were removed and weighed. For each animal, a lesion was fixed in 4% paraformaldehyde in PBS (pH 7.4) for 24 h at 4 °C. Fixed specimens were embedded in paraffin and cut into 4- μ m-thick sections. A standard hematoxylin-eosin procedure was used to confirm the presence of endometrial glands and stroma in the ectopic tissue and to count the number of blood vessels. Other 4- μ m-sections were prepared for cell proliferation study. Another lesion was placed at -20 °C in RNAhold[®] (TransGen Biotech[®] Co., Ltd., Beijing, China) for RT-qPCR studies. The third lesion was kept at -80 °C for protein extraction.

Estradiol determination. An electrochemiluminescence immunoassay (ECLIA) kit specific for estradiol (Elesys Estradiol III, Roche Diagnostics International Ltd., Mannheim, Germany) was used, according to manufacturer's instructions. The lower and upper detection limits were 5 and 3000 pg/mL, respectively. All measurements were performed in duplicate. Estradiol levels in the peritoneal fluid were expressed in pg/mL.

Immunohistochemistry of PCNA. Proliferating cell nuclear antigen (PCNA) is a nuclear protein involved in cellular DNA replication; therefore, it was evaluated in endometriotic-like lesions of untreated and TM-treated mice by immunohistochemistry. Tissue sections from six different animals per experimental group were deparaffinized in xylene and rehydrated in a graded series of ethyl alcohols. For antigen retrieval, slides were transferred to a glass staining jar filled with 0.01 M sodium citrate buffer (pH 6.0), which was placed in a microwave oven for 10 min on the highest power. Endogenous peroxidase was blocked with 3% H₂O₂ for 30 min. All the sections were blocked with 4% BSA in 1 \times PBS for 2 h at room temperature in a humid chamber and then incubated with a polyclonal rabbit anti-PCNA antibody (1:150; FL-261, Santa Cruz Biotechnology, CA, USA) overnight at 4 °C. For negative controls, the primary antibody was replaced with 1% BSA in 1 \times PBS. Subsequently, sections were incubated with a biotinylated goat anti-rabbit IgG antibody (1:500; B8895, Sigma-Aldrich, St Louis, MO, USA) for 1 h at room temperature. Then, they were incubated with HRP-conjugated streptavidin (VectorLabs, Burlingame, CA, USA) for 30 min at room temperature. Diaminobenzidine (DAB) was used as substrate and incubated for 5 min (Cell Marque, CA, USA). Finally, tissue sections were counterstained with hematoxylin, dehydrated with graded alcohols, cleared in xylene, and properly mounted. PCNA-positive cells were identified by the presence of brown nuclear reactivity. Their percentage was established by two different operators at 1000 \times under optical light microscopy (Olympus, Japan) by analyzing six representative fields per section. The total positive cell percentage was calculated per slide and was used to obtain the mean of each experimental group.

Mean blood vessel count. Blood vessels of different calibers were counted in sections of endometriotic-like lesions stained with hematoxylin-eosin using an optical light microscope (Olympus, Japan) at 400 \times . Tissue sections from six different animals per experimental group and between 6 and 8 fields per section were observed by two different operators. Blood vessels identified in each section were reviewed and approved by a pathologist. Results were expressed as the mean blood vessel count per field for the KO EDT and KO EDT+TM groups.

Quantitative reverse transcription PCR (RT-qPCR). RT-qPCR was performed to analyze the gene expression of the following genes: *Vegfa*, *Fgf2*, and Platelet-Derived Growth Factor B (*Pdgfb*). Total RNA was isolated from endometriotic-like lesions using TRIzol[®] reagent (Thermo Fisher Scientific, Inc., Waltham, MA, USA). RNA samples were quantified using an EPOCH[™] microplate spectrophotometer (BioTek Instruments, Inc., Vermont, USA). All high-purity and intact RNA samples were treated with RQ1 RNase-Free DNase (Promega). Total RNA (1 μ g) was reverse-transcribed using Transcriptor First Strand cDNA Synthesis Kit (Roche Diagnostics International Ltd., Mannheim, Germany) and stored at -20 °C, following manufacturer's guidelines. For qPCR, cDNA was amplified in an ABI PRISM[®] 7500 Instrument (Applied Biosystems, USA), using FastStart[™] Universal SYBR[®] Green Master (Roche Diagnostics International Ltd., Mannheim, Germany). The reaction mixture consisted of 2 \times FastStart[™] Universal SYBR[®] Green Master Mix, cDNA, forward primer (10 μ M),

Gene	Sequences (5'–3')	GenBank access number	Amplicon (bp)
<i>Vegfa</i>	Forward: CACTTCCAGAAACACGACAAAC	NM_001025250.3	95
	Reverse: TGGAACCGGCATCTTATCTC		
<i>Fgf2</i>	Forward: GGCATCACCTCGCTTCC	NM_008006.2	97
	Reverse: CGCCGTTCTTGCAGTAGAG		
<i>Pdgfb</i>	Forward: GAGTGTGGCAGGGTTATTT	NM_011057.4	105
	Reverse: GAATCAGGCATCGAGACAGAC		
<i>Rn18s</i>	Forward: CTGAGAAACGGCTACCACATC	NR_003278.3	107
	Reverse: GCCTCGAAAGAGTCTGTATTG		

Table 1. Primer gene symbols, sequences, GenBank access numbers, and sizes of amplicons.

reverse primer (10 μ M), and nuclease-free water. All primers are described in Table 1. PCR cycling conditions were 95 °C, 10 min; 40 cycles at 95 °C, 15 s; 60 °C, 1 min. The relative expression was calculated using the $2^{-\Delta\Delta Ct}$ method⁵⁴. All experiments were performed in duplicate. *Rn18s* (18S ribosomal RNA): internal reference gene.

Antioxidant enzyme activities. Proteins from lesions were extracted in 100 μ L RIPA buffer (Thermo Fisher Scientific Inc., Waltham, MA, USA) and quantified according to Bradford method⁵⁵, as previously described²⁶. To measure superoxide dismutase (SOD) activity, the pyrogallol autoxidation method was used, monitoring the change in absorbance at 420 nm per min. One unit of the enzyme was expressed as the amount of SOD that inhibits 50% of pyrogallol autoxidation⁵⁶. The catalase (CAT) activity was determined by measuring the decrease in H₂O₂ absorption at 240 nm, in which one CAT unit is the amount of enzyme required to decompose 1 μ M of H₂O₂/min⁵⁷. The glutathione peroxidase (GPX) activity was determined by following NADPH oxidation at 340 nm⁵⁸. All readings were carried out using a Shimadzu 1800 UV–Visible spectrophotometer. The results were expressed as units of enzyme activity per milligram of protein (U/mg protein). All measurements were performed in duplicate.

Measurement of MDA. The levels of malondialdehyde (MDA), the end product of lipid peroxidation, were determined according to the method described by Draper and Hadley⁵⁹. This method was based on the reaction of MDA with thiobarbituric acid (TBA). 1,1,3,3-tetraethoxypropane was used as a standard for the calibration curve, and the results were expressed as μ mol MDA/mg protein. All measurements were performed in duplicate.

Statistical analysis. Statistical analysis was performed using GraphPad Prism 5.0 software (GraphPad Software Inc., San Diego, CA, USA). Values were presented as the mean \pm SEM. Differences between groups were analyzed using a two-tailed unpaired Student's *t* test or one-way ANOVA followed by Tukey's multiple comparison test (when appropriate). For the correlation analysis, the normality of data was assessed with the Shapiro–Wilk test, and Spearman's correlation method was applied. Differences were statistically significant when $P < 0.05$.

Data availability

Data used to support the findings of this study are available upon request from the corresponding authors (M.C. and M.B.D.).

Received: 16 August 2022; Accepted: 14 June 2023

Published online: 26 June 2023

References

- Taylor, H. S., Kotlyar, A. M. & Flores, V. A. Endometriosis is a chronic systemic disease: Clinical challenges and novel innovations. *Lancet* **397**, 839–852. [https://doi.org/10.1016/S0140-6736\(21\)00389-5](https://doi.org/10.1016/S0140-6736(21)00389-5) (2021).
- Warzecha, D., Szymusik, I., Wielgos, M. & Pietrzak, B. The impact of endometriosis on the quality of life and the incidence of depression: A cohort study. *Int. J. Environ. Res. Public Health* **17**, 3641. <https://doi.org/10.3390/ijerph17103641> (2020).
- Richter, O. N., Dorn, C., Rösing, B., Flaskamp, C. & Ulrich, U. Tumor necrosis factor alpha secretion by peritoneal macrophages in patients with endometriosis. *Arch. Gynecol. Obstet.* **271**, 143–147. <https://doi.org/10.1007/s00404-003-0591-9> (2005).
- Braun, D. P., Ding, J. & Dmowski, W. P. Peritoneal fluid-mediated enhancement of eutopic and ectopic endometrial cell proliferation is dependent on tumor necrosis factor- α in women with endometriosis. *Fertil. Steril.* **78**, 727–732. [https://doi.org/10.1016/S0015-0282\(02\)03318-6](https://doi.org/10.1016/S0015-0282(02)03318-6) (2002).
- Vallcaneras, S. *et al.* TNFRp55 deficiency promotes the development of ectopic endometriotic-like lesions in mice. *J. Endocrinol.* **234**, 269–278. <https://doi.org/10.1530/JOE-17-0236> (2017).
- Delsouc, M. B. *et al.* Endometriosis progression in tumor necrosis factor receptor p55-deficient mice: Impact on oxidative/nitrosative stress and metallomic profile. *J. Trace Elem. Med. Biol.* **52**, 157–165. <https://doi.org/10.1016/j.jtemb.2018.12.013> (2019).
- Naserian, S. *et al.* The TNF/TNFR2 signaling pathway is a key regulatory factor in endothelial progenitor cell immunosuppressive effect. *Cell Commun. Signal.* **18**, 1–14. <https://doi.org/10.1186/s12964-020-00564-3> (2020).
- Sheng, Y., Li, F. & Qin, Z. TNF receptor 2 makes tumor necrosis factor a friend of tumors. *Front. Immunol.* **9**, 1–9. <https://doi.org/10.3389/fimmu.2018.01170> (2018).
- Takahashi, H., Yoshimatsu, G. & Faustman, D. L. The roles of TNFR2 signaling in cancer cells and the tumor microenvironment and the potency of TNFR2 targeted therapy. *Cells* **11**, 1952. <https://doi.org/10.3390/cells11121952> (2022).
- Gough, P. & Myles, I. A. Tumor necrosis factor receptors: Pleiotropic signaling complexes and their differential effects. *Front. Immunol.* **11**, 585880. <https://doi.org/10.3389/fimmu.2020.585880> (2020).

11. Rojas-Cartagena, C., Appleyard, C. B., Santiago, O. I. & Flores, I. Experimental intestinal endometriosis is characterized by increased levels of soluble TNFRSF1B and downregulation of Tnfrsf1a and Tnfrsf1b gene expression. *Biol. Reprod.* **73**, 1211–1218. <https://doi.org/10.1095/biolreprod.105.044131> (2005).
12. Boric, M. A. *et al.* TNF system in eutopic endometrium from women with endometriosis. *Open J. Obstet. Gynecol.* <https://doi.org/10.4236/ojog.2013.32051> (2013).
13. Salmeri, F. M. *et al.* Behavior of tumor necrosis factor- α and tumor necrosis factor receptor 1/tumor necrosis factor receptor 2 system in mononuclear cells recovered from peritoneal fluid of women with endometriosis at different stages. *Reprod. Sci.* **22**, 165–172. <https://doi.org/10.1177/1933719114536472> (2015).
14. Ghersa, F. *et al.* Reduced inflammatory state promotes reinnervation of endometriotic-like lesions in TNFRp55 deficient mice. *Mol. Hum. Reprod.* **25**, 385–396. <https://doi.org/10.1093/molehr/gaz026> (2019).
15. Turgut, A. I. *et al.* Copper, ceruloplasmin and oxidative stress in patients with advanced-stage endometriosis. *Eur. Rev. Med. Pharmacol. Sci.* **17**, 1472–1478 (2013).
16. Pollack, A. Z. *et al.* Trace elements and endometriosis: The ENDO Study. *Reprod. Toxicol.* **42**, 41–48. <https://doi.org/10.1016/j.reprotox.2013.05.009> (2013).
17. Scutiero, G. *et al.* Oxidative stress and endometriosis: A systematic review of the literature. *Oxid. Med. Cell. Longev.* <https://doi.org/10.1155/2017/7265238> (2017).
18. Lelièvre, P., Sancey, L., Coll, J.-L., Deniaud, A. & Busser, B. The multifaceted roles of copper in cancer: A trace metal element with dysregulated metabolism, but also a target or a bullet for therapy. *Cancers (Basel)* **12**, 3594. <https://doi.org/10.3390/cancers12123594> (2020).
19. Li, Y. Copper homeostasis: Emerging target for cancer treatment. *IUBMB Life* **72**, 1900–1908. <https://doi.org/10.1002/iub.2341> (2020).
20. Wada, H. G., Fok, K. S., Fendly, B. M., Chiang, N. Y. & Sussman, H. H. Activation of TNF-R1 receptor in the presence of copper kills TNF resistant CEM leukemic T cells. *J. Cell. Physiol.* **161**, 597–605. <https://doi.org/10.1002/jcp.1041610324> (1994).
21. Liu, H. *et al.* Copper induces oxidative stress and apoptosis in the mouse liver. *Oxid. Med. Cell. Longev.* <https://doi.org/10.1155/2020/1359164> (2020).
22. Martin, M. B. *et al.* Estrogen-like activity of metals in MCF-7 breast cancer cells. *Endocrinology* **144**, 2425–2436. <https://doi.org/10.1210/en.2002-221054> (2003).
23. Soni, R. K. *et al.* Effect of in vitro copper supplementation on granulosa cell estradiol synthesis and associated genes. *Indian J. Anim. Res.* **52**, 652–657. <https://doi.org/10.18805/ijar.B-3396> (2018).
24. Platteeuw, L. & D'Hooghe, T. Novel agents for the medical treatment of endometriosis. *Curr. Opin. Obstet. Gynecol.* **26**, 243–252. <https://doi.org/10.1097/gco.000000000000084> (2014).
25. Rogers, P. A. *et al.* WES/WERF consortium for research priorities in endometriosis. Research priorities for endometriosis. *Reprod. Sci.* **24**, 202–226. <https://doi.org/10.1177/1933719116654991> (2017).
26. Delsouc, M. B. *et al.* Antiproliferative and antiangiogenic effects of ammonium tetrathiomolybdate in a model of endometriosis. *Life Sci.* **287**, 120099. <https://doi.org/10.1016/j.lfs.2021.120099> (2021).
27. Aggarwal, A. & Bhatt, M. Advances in treatment of Wilson disease. *Tremor and Other Hyperkinetic Movements*, vol. 8 <https://doi.org/10.7916/D841881D> (2018).
28. Pan, Q. *et al.* Copper deficiency induced by tetrathiomolybdate suppresses tumor growth and angiogenesis. *Cancer Res.* **62**, 4854–4859 (2002).
29. Brewer, G. J. The promise of copper lowering therapy with tetrathiomolybdate in the cure of cancer and in the treatment of inflammatory disease. *J. Trace Elem. Med. Biol.* **28**, 372–378. <https://doi.org/10.1016/j.jtemb.2014.07.015> (2014).
30. Flores, I. *et al.* Molecular profiling of experimental endometriosis identified gene expression patterns in common with human disease. *Fertil. Steril.* **87**, 1180–1199. <https://doi.org/10.1016/j.fertnstert.2006.07.1550> (2007).
31. Vanamee, E. S. & Faustman, D. L. TNFR2: A novel target for cancer immunotherapy. *Trends Mol. Med.* **23**, 1037–1046. <https://doi.org/10.1016/j.molmed.2017.09.007> (2017).
32. Rivas, M. A. *et al.* TNF α acting on TNFR1 promotes breast cancer growth via p42/P44 MAPK, JNK, Akt and NF- κ B-dependent pathways. *Exp. Cell Res.* **314**, 509–529. <https://doi.org/10.1016/j.yexcr.2007.10.005> (2008).
33. İslimye, M. *et al.* Regression of endometrial autografts in a rat model of endometriosis treated with etanercept. *Eur. J. Obstet. Gynecol. Reprod. Biol.* **159**, 184–189. <https://doi.org/10.1016/j.ejogrb.2011.06.029> (2011).
34. Barthel, A., Ostrakhovitch, E. A., Walter, P. L., Kampkötter, A. & Klotz, L.-O. Stimulation of phosphoinositide 3-kinase/Akt signaling by copper and zinc ions: Mechanisms and consequences. *Arch. Biochem. Biophys.* **463**, 175–182. <https://doi.org/10.1016/j.abb.2007.04.015> (2007).
35. Turski, M. L. *et al.* A novel role for copper in Ras/mitogen-activated protein kinase signaling. *Mol. Cell. Biol.* **32**, 1284–1295. <https://doi.org/10.1128/MCB.05722-11> (2012).
36. Klevay, L. M. & Christopherson, D. M. Copper deficiency halves serum dehydroepiandrosterone in rats. *J. Trace Elem. Med. Biol.* **14**, 143–145. [https://doi.org/10.1016/S0946-672X\(00\)80002-4](https://doi.org/10.1016/S0946-672X(00)80002-4) (2000).
37. McKinnon, B. D., Kocbek, V., Nirgianakis, K., Bersinger, N. A. & Mueller, M. D. Kinase signalling pathways in endometriosis: Potential targets for non-hormonal therapeutics. *Hum. Reprod. Update* **22**, 382–403. <https://doi.org/10.1093/humupd/dmv060> (2016).
38. Xu, M., Casio, M., Range, D. E., Sosa, J. A. & Counter, C. M. Copper chelation as targeted therapy in a mouse model of oncogenic BRAF-driven papillary thyroid cancer. *Clin. Cancer Res.* **24**, 4271–4281. <https://doi.org/10.1158/1078-0432.CCR-17-3705> (2018).
39. Brady, D. C., Crowe, M. S., Greenberg, D. N. & Counter, C. M. Copper chelation inhibits BRAFV600E-driven melanomagenesis and counters resistance to BRAFV600E and MEK1/2 inhibitors. *Cancer Res.* **77**, 6240–6252. <https://doi.org/10.1158/0008-5472.CAN-16-1190> (2017).
40. Laschke, M. W. & Menger, M. D. Basic mechanisms of vascularization in endometriosis and their clinical implications. *Hum. Reprod. Update* **24**, 207–224. <https://doi.org/10.1093/humupd/dmy001> (2018).
41. Laschke, M. W., Elitzsch, A., Vollmar, B., Vajkoczy, P. & Menger, M. D. Combined inhibition of vascular endothelial growth factor (VEGF), fibroblast growth factor and platelet-derived growth factor, but not inhibition of VEGF alone, effectively suppresses angiogenesis and vessel maturation in endometriotic lesions. *Hum. Reprod.* **21**, 262–268. <https://doi.org/10.1093/humrep/dei308> (2006).
42. Brewer, G. J., Ullenbruch, M. R., Dick, R., Olivarez, L. & Phan, S. H. Tetrathiomolybdate therapy protects against bleomycin-induced pulmonary fibrosis in mice. *J. Lab. Clin. Med.* **141**, 210–216. <https://doi.org/10.1067/mlc.2003.20> (2003).
43. Wei, H., Zhang, W. J., LeBoeuf, R. & Frei, B. Copper induces—and copper chelation by tetrathiomolybdate inhibits—endothelial activation in vitro. *Redox Rep.* **19**, 40–48. <https://doi.org/10.1179/1351000213Y.0000000070> (2014).
44. Kumar, P. *et al.* Tetrathiomolybdate inhibits head and neck cancer metastasis by decreasing tumor cell motility, invasiveness and by promoting tumor cell anoikis. *Mol. Cancer* **9**, 1–11. <https://doi.org/10.1186/1476-4598-9-206> (2010).
45. Kim, K. K., Lange, T. S., Singh, R. K., Brard, L. & Moore, R. G. Tetrathiomolybdate sensitizes ovarian cancer cells to anticancer drugs doxorubicin, fenretinide, 5-fluorouracil and mitomycin C. *BMC Cancer* **12**, 147. <https://doi.org/10.1186/1471-2407-12-147> (2012).
46. Uegaki, T. *et al.* Inhibitor of apoptosis proteins (IAPs) may be effective therapeutic targets for treating endometriosis. *Hum. Reprod.* **30**, 149–158. <https://doi.org/10.1093/humrep/deu288> (2015).

47. Yu, H., Lin, L., Zhang, Z., Zhang, H. & Hu, H. Targeting NF- κ B pathway for the therapy of diseases: Mechanism and clinical study. *Signal Transduct. Target. Ther.* **5**, 1–23. <https://doi.org/10.1038/s41392-020-00312-6> (2020).
48. Denoyer, D., Clatworthy, S. A. S. & Cater, M. A. *Copper Complexes in Cancer Therapy. Metal Ions in Life Sciences* vol. 18. <https://doi.org/10.1515/9783110470734-016> (2018).
49. Juarez, J. C. *et al.* Superoxide dismutase 1 (SOD1) is essential for H₂O₂-mediated oxidation and inactivation of phosphatases in growth factor signaling. *Proc. Natl. Acad. Sci. U.S.A.* **105**, 7147–7152. <https://doi.org/10.1073/pnas.0709451105> (2008).
50. Ngó, C. *et al.* Reactive oxygen species controls endometriosis progression. *Am. J. Pathol.* **175**, 225–234. <https://doi.org/10.2353/ajpath.2009.080804> (2009).
51. Cacciottola, L., Donnez, J. & Dolmans, M.-M. Can endometriosis-related oxidative stress pave the way for new treatment targets?. *Int. J. Mol. Sci.* **22**, 7138. <https://doi.org/10.3390/ijms22137138> (2021).
52. Tokuda, E., Okawa, E., Watanabe, S., Ono, S. & Marklund, S. L. Dysregulation of intracellular copper homeostasis is common to transgenic mice expressing human mutant superoxide dismutase-1s regardless of their copper-binding abilities. *Neurobiol. Dis.* **54**, 308–319. <https://doi.org/10.1016/j.nbd.2013.01.001> (2013).
53. Brewer, G. J. *et al.* Treatment of metastatic cancer with tetrathiomolybdate, an anticopper, antiangiogenic agent: Phase I study. *Clin. Cancer Res.* **6**, 1–10 (2000).
54. Livak, K. J. & Schmittgen, T. D. Analysis of relative gene expression data using real-time quantitative PCR and the 2^{- $\Delta\Delta$ CT} method. *Methods* **25**, 402–408. <https://doi.org/10.1006/meth.2001.1262> (2001).
55. Bradford, M. M. A rapid and sensitive method for the quantitation of microgram quantities of protein utilizing the principle of protein-dye binding. *Anal. Biochem.* **72**, 248–254. <https://doi.org/10.1006/abio.1976.9999> (1976).
56. Marklund, S. & Marklund, G. Involvement of the superoxide anion radical in the autoxidation of pyrogallol and a convenient assay for superoxide dismutase. *Eur. J. Biochem.* **47**, 469–474. <https://doi.org/10.1111/j.1432-1033.1974.tb03714.x> (1974).
57. Aebi, H. Catalase in vitro. In *Methods in Enzymology* Vol. 105 121–126 (Elsevier, 1984). [https://doi.org/10.1016/s0076-6879\(84\)05016-3](https://doi.org/10.1016/s0076-6879(84)05016-3).
58. Flohé, L. & Günzler, W. A. Assays of glutathione peroxidase. In *Methods in Enzymology* Vol. 105 114–120 (Elsevier, 1984). [https://doi.org/10.1016/s0076-6879\(84\)05015-1](https://doi.org/10.1016/s0076-6879(84)05015-1).
59. Draper, H. H. & Hadley, M. Malondialdehyde determination as index of lipid peroxidation. In *Methods in Enzymology* Vol. 186 421–431 (Elsevier, 1990). [https://doi.org/10.1016/0076-6879\(90\)86135-i](https://doi.org/10.1016/0076-6879(90)86135-i).

Acknowledgements

This work was supported by grants from Universidad Nacional de San Luis (UNSL), Argentina [PROICO 02-0720] and the Institutional Research Program [Resolution No. 238/21]. Also, this work was funded by the Consejo Nacional de Investigaciones Científicas y Técnicas (CONICET), Argentina [PIP 2021-2023/00969], and the Agencia Nacional de Promoción Científica y Tecnológica (ANPCyT), Argentina [PICT-2020-SERIEA-03793]. We thank Gustavo Cramero, Director of Laboratorio de Análisis Clínicos (LAC, Tunuyán, Mendoza, Argentina), and Pablo Pacheco (INQUISAL-CONICET, San Luis, Argentina) for their advice in the estradiol and Cu determination, respectively. We thank Silvana Semino, a pathologist (UNCuyo, Mendoza, Argentina), for corroborating the analyzes performed on histological sections of endometriotic-like lesions. We would also like to thank Carolina Mirallas from the Gabinete de Asesoramiento en Escritura Científica en Inglés (GAECI) for the language revision of this manuscript. S.S.V. and M.C. are members of the CIC-CONICET-Argentina. This work is part of the Doctoral thesis of Rocío Ayelem Conforti.

Author contributions

R.A.C., methodology, investigation, visualization, formal analysis, writing—original draft. M.B.D., conceptualization, methodology, investigation, visualization, formal analysis, writing—review and editing. A.S.Z., methodology, investigation. S.S.V., methodology, investigation. M.C., conceptualization, supervision, funding acquisition, writing—review and editing. All authors reviewed the manuscript.

Competing interests

The authors declare no competing interests.

Additional information

Supplementary Information The online version contains supplementary material available at <https://doi.org/10.1038/s41598-023-37031-1>.

Correspondence and requests for materials should be addressed to M.B.D. or M.C.

Reprints and permissions information is available at www.nature.com/reprints.

Publisher's note Springer Nature remains neutral with regard to jurisdictional claims in published maps and institutional affiliations.



Open Access This article is licensed under a Creative Commons Attribution 4.0 International License, which permits use, sharing, adaptation, distribution and reproduction in any medium or format, as long as you give appropriate credit to the original author(s) and the source, provide a link to the Creative Commons licence, and indicate if changes were made. The images or other third party material in this article are included in the article's Creative Commons licence, unless indicated otherwise in a credit line to the material. If material is not included in the article's Creative Commons licence and your intended use is not permitted by statutory regulation or exceeds the permitted use, you will need to obtain permission directly from the copyright holder. To view a copy of this licence, visit <http://creativecommons.org/licenses/by/4.0/>.

© The Author(s) 2023